[8]This assumption is appropriate for the sputtered-atom kinetic energy considered in Fig. 1. See Ref. 5.

[9]For atoms like oxygen that get deep into the surface electron gas, the dominant variation of $\epsilon_a(z)$ is exponential, but the heavier alkalis tend to be adsorbed at large distances from the surface, outside of which Eq. (2) is expected to be adequate.

[10]M. L. Yu, Phys. Rev. Lett. 47, 1325 (1981).

[11]N. D. Lang and W. Kohn, Phys. Rev. B 7, 3541 (1973).

[12]Adding the difference between Cs and Na radii to a calculated Na equilibrium position (Ref. 6) gives the Cs equilibrium position. Calculations for this position following Ref. 6 give Δ_0 and use of the results of Ref. 11 gives z_{im}.

[13]Let $\psi(z)$ be the z-dependent part of the single-particle wave function outside the bare surface. The definition of $\Delta(z)$ in terms of the square of a metal-adatom matrix element (Refs. 2–5) suggests that very roughly $\Delta(z)/\Delta_0 \sim |\psi(z)|^2/|\psi(0)|^2$. Equation (1) thus corresponds to $\psi(z)$ exhibiting pure exponential decay, which would be true if the electron potential were constant. In fact, the potential must have an image form away from the immediate surface region. We can consider extracting an effective γ value for use in our equations by solving the one-particle equation for $\psi(z)$ with an image potential, and obtaining the ratio $|\psi(z_c)|^2/|\psi(0)|^2$. The energy value we use in this equation is $\epsilon_a(z_c) = \varphi$. We thus neglect any energy dependence of Δ_0 over the energy range of interest [since $\epsilon_a(0) \neq \epsilon_a(z_c)$], but this should be unimportant. This gives a γ that ranges from 0.7 bohr^{-1} for $\varphi \sim 3$ eV to 1.1 bohr^{-1} for $\varphi \geq I = 3.9$ eV (corresponding to $z_c \to \infty$). Since the larger values of φ correspond to large values of z_c, for which $P^+ \cong 1$ independent of the exact value of γ, the lower end of the range of γ values gives a better description of the results if we wish to pick a single value to describe them all. If we evaluate our equations at each φ using the γ value obtained for that φ, we obtain a curve that differs only slightly from that which takes a constant $\gamma = 0.7$ bohr^{-1}.

Microscopic Theory of the Temperature-Pressure Phase Diagram of Iron

H. Hasegawa
The Institute for Solid State Physics, The University of Tokyo, Roppongi, Tokyo, Japan

and

D. G. Pettifor
Department of Mathematics, Imperial College, London, England

(Received 19 August 1982)

The free energy of bcc, fcc, and hcp iron has been calculated as a function of temperature and pressure within the single-site spin-fluctuation theory of band magnetism, which has been developed recently by Hubbard and Hasegawa. The simple theory can account for the occurrence of the α, γ, δ, and ϵ phases in the T-P phase diagram of iron, the phase transitions being driven by the magnetic contributions to the free energy.

PACS numbers: 81.30.Bx, 75.10.Lp, 75.50.Bb

There have been many attempts[1-6] to understand the phase diagram[7] of iron, because it is central to the behavior of a most important class of alloys, the steels. The unique property of iron of transforming from the high-temperature close-packed fcc γ phase to the low-temperature bcc α phase (see the inset of Fig. 1) is used in steel technology for producing a wide variety of microstructures with corresponding different physical characteristics. The reason for the appearance of the *closed-packed* γ phase at the higher temperatures remains, however, controversial. On the one hand, several authors[2,3] have argued that the γ-phase stability arises from the *vibrational* contribution to the free energy by assuming that the Debye temperature of the γ phase is 25% smaller than that of the α phase. On the other hand, Kaufman *et al.*[4] have claimed that it arises from the very unusual *magnetic* behavior of γ iron, proposing the phenomenological two-γ-state model which provides the additional entropy required to stabilize the γ phase. Yet, when discussing the hcp ϵ phase shown in Fig. 1, Kaufman and colleagues[5] required an additional stabilizing contribution and assumed that the Debye temperature of the close-packed ϵ phase is 15% lower than that of either the α or γ phase. Since there was no *a priori* theoretical justification for either the *phenomenological* two-γ-state hypothesis or the lower Debye temperature[6] of the close-packed phases, the question of the origin of the α, γ, δ, and ϵ phases remained open. In this Letter we present the first *microscopic* explanation of the phase diagram of iron by applying the itinerant-

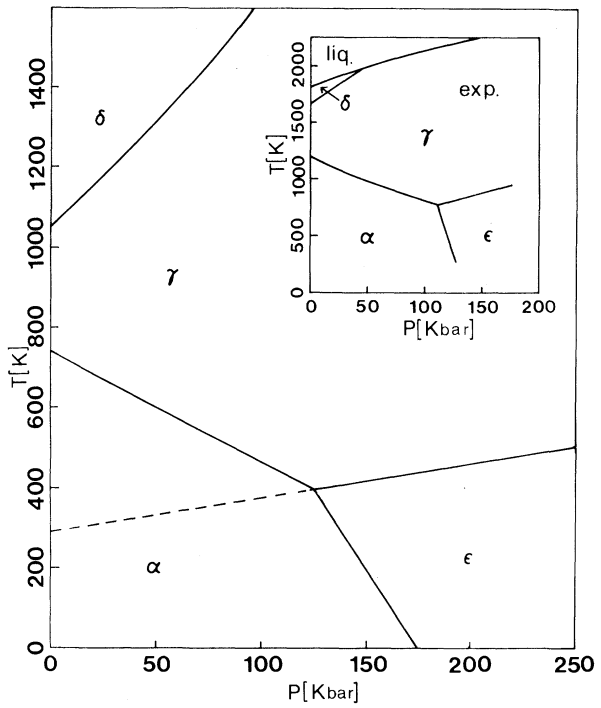

FIG. 1. The calculated T-P phase diagram of iron, the inset showing the observed one (Ref. 7). The dashed line gives the metastable ϵ-γ boundary. The α-ϵ boundary is obtained by interpolating between the triple point and $P_c^{\alpha\epsilon}$ at $T=0$ K.

electron theory of band magnetism which has recently been extended to finite temperatures with some success by Hasegawa[8,9] and Hubbard.[10] We will see that the phase transitions in iron are driven by the magnetic contributions to the free energy.

The cohesive and structural properties[11] of the transition metals in their ground state are determined by the bonding of the valence d electrons. We, therefore, write the Helmholz free energy per atom in the form

$$F(V,T)=F_B(V,T)+F_R(V), \tag{1}$$

where F_B is the band free energy of the itinerant d electrons and F_R is the repulsive contribution that counters the attractive d-band term. We neglect the vibrational contribution in the present simple model, the consequences of which will be discussed later.

The band free energy F_B is evaluated within the single-site spin-fluctuation theory[8-10] of itinerant magnetism, which extends Stoner theory to include the effect of spin fluctuations at finite temperatures by using the functional integral method within the static approximation. It is a *mean-field* theory in which short-range magnetic order (SRMO) is neglected, so that the paramagnetic state above the Curie temperature T_C is regarded[12] as a collection of *disordered* moments which may point either up or down in an Ising-type manner. The problem is formally analogous to that of a disordered alloy and may, therefore, be treated within the coherent-potential approximation (CPA).[13] Hasegawa[8] has shown that in bcc iron disordered local moments can be sustained self-consistently within a band framework above T_C, which is in direct contrast to Stoner theory where the exchange field and hence the local moment have collapsed. However, unlike the conventional Ising and Heisenberg models of magnetism, the *amplitude* of the local moment in the most recent Hubbard[10] and Hasegawa[9] theory is not fixed but fluctuates with temperature as local exchange fields of differing magnitude become thermally populated. We will see that this leads in the case of the close-packed fcc and hcp lattices to temperature-induced local moments.[14]

Within the single-band spin-fluctuation theory of Hubbard[10] and Hasegawa[9] F_B may be written by

$$F_B=E-TS, \tag{2}$$

where

$$E=(U/4)\langle\zeta^2\rangle+\int d\epsilon f(\epsilon)\epsilon\sum_\sigma\rho_\sigma(\epsilon), \tag{3}$$

$$S=-\int d\epsilon\sum_\sigma\rho_\sigma(\epsilon)\{f\ln f+(1-f)\ln(1-f)\}-\langle\ln C(\zeta)\rangle, \tag{4}$$

$$\rho_\sigma(\epsilon)=(-1/\pi)\mathrm{Im}F_\sigma(\epsilon), \tag{5}$$

$$F_\sigma(\epsilon)=\int d\omega\,\rho_0(\omega)/\{\epsilon-\Sigma_\sigma(\epsilon)-\omega\}. \tag{6}$$

In Eqs. (2)–(6), U is the electron-electron interaction and $f(\epsilon)$ is the Fermi distribution function, which is treated in the low-temperature approximation. $\rho_\sigma(\epsilon)$ is the usual[13] CPA density of states per atom for σ-spin electrons that depends on the coherent potential $\Sigma_\sigma(\epsilon)$ and the unperturbed (i.e., nonmagnetic) density of states $\rho_0(\omega)$ for a single band. The angular brackets denote the average over the "alloy" concentration $C(\zeta)$ of local exchange fields ζ which are populated[9,10] at a given temperature T. It follows from functional integral theory that the mean and rms values of the local moment are given by $\langle m\rangle=\langle\zeta\rangle$ and $\langle m^2\rangle^{1/2}=\{\langle\zeta^2\rangle-2T/U\}^{1/2}$. Therefore, the internal energy E reduces to the usual Stoner expression at $T=0$ K.

We have solved these self-consistency equations[9] for the three different crystal lattices bcc, fcc, and hcp using the corresponding tight-bind-

ing d-band densities of states $\rho_0(\epsilon)$.[15,16] Iron was taken to have $1.4 = 7.0/5$ d electrons, the factor 5 being the orbital degeneracy. An effective d-band width, W,[11] of 0.45 Ry (Ref. 17) and U of 4.8 eV (Ref. 18) were used. It is assumed that U is volume independent[16] and W is proportional to the $\frac{5}{3}$ power of volume.[19]

The repulsive contribution to the energy of transition metals[11] has not yet been successfully separated into volume- and structure-dependent components, and so we have assumed a semiempirical Lennard-Jones-type behavior, namely,

$$F_R = A^i/S^{12}, \tag{7}$$

where S is the Wigner-Seitz radius and A^i is a structure-dependent constant ($i = \alpha$, γ, or ϵ). A^α is chosen to fit the observed equilibrium Wigner-Seitz radius of 2.66 a.u. (S_0) of ferromagnetic α iron at $T = 0$ K. A^γ and A^ϵ are adjusted to give the α/γ and ϵ/γ transformations in the vicinity of the Curie temperature T_C and at $0.4T_C$, respectively, at zero pressure (see Fig. 1). We find $A^\gamma/A^\alpha = 0.9849$, $A^\epsilon/A^\alpha = 0.9916$, and $A^\alpha/S^{12} = 0.3574$ eV/atom. Equations (1)–(7) determine completely the behavior of the Gibbs free energy, $G = F + PV$, as a function of temperature and pressure.

The structural behavior of iron at *zero temperature* is well understood[11,16-18] within Stoner theory. In the *nonmagnetic* state the internal energy E is given by Eq. (3) as an energy integral involving the density of states $\rho_0(\epsilon)$. The resulting contribution as a function of band filling accounts[11,20] for the well-known hcp → bcc → hcp → fcc structure trend across the nonmagnetic $4d$ and $5d$ transition-metal series. For iron, this nonmagnetic band-structure contribution gives[20] hcp the most stable and bcc the least-stable crystal structure, which is consistent with the nonmagnetic isovalent $4d$ and $5d$ elements Ru and Os being hcp. However, the bcc density of states has a very large peak in the vicinity of the iron Fermi level, which is not present in the close-packed structures.[11,18] This allows $3d$ α iron to satisfy the Stoner criterion $U\rho_0(\epsilon_F) > 1$ for the onset of ferromagnetism, whereas γ and ϵ iron are unable to do so at their equilibrium volumes.[21] The resulting *ferromagnetic* energy[11] contribution of bcc iron is sufficient to stabilize the α phase with respect to the close-packed structures at $T = 0$ K (cf. Fig. 2). Under pressure, however, the magnetic energy decreases as the bands broaden and the bcc α phase transforms[18] to the hcp ϵ phase (cf. Fig. 1).

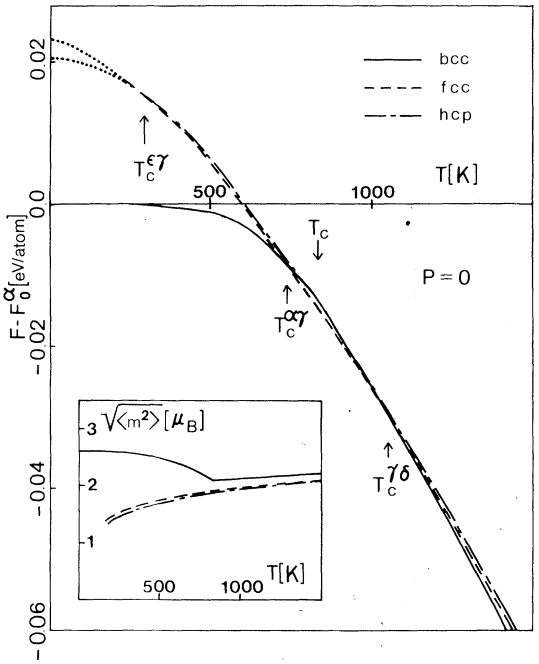

FIG. 2. The calculated free energies (Ref. 22) of bcc, fcc, and hcp iron at zero pressure with the inset showing the temperature dependence of their effective rms local magnetic moments. Below about 200 K the curves are shown dotted as the static approximation breaks down in the vicinity of absolute zero due to the neglect of dynamic quantum fluctuations.

The calculated free-energy curves[22] of bcc, fcc, and hcp iron (relative to the ground-state energy of α iron) are shown in Fig. 2 as a function of temperature at *zero pressure*. We must stress at the outset that the choice of the repulsive coefficients A^i does not affect the shape of these curves, which is determined by the temperature dependence of the band contribution F_B. The strong curvature displayed by the bcc free energy above 500 K reflects the rapid buildup in magnetic entropy as the ferromagnetically aligned moments disorder as the calculated Curie temperature of 830 K is approached from below. As shown in the inset the rms local moment of α iron[23] decreases as the moments disorder and then increases slowly above T_C as the amplitude fluctuations build up. On the other hand, the close-packed structures, which have zero moment[21] at $T = 0$ K, show temperature-induced local-moment behavior which is similar to that predicted by the phenomenological 2γ-state model.[4] It is accompanied by a rapid buildup in the magnetic entropy through the $\langle \ln C \rangle$ term in Eq. (4), which is sufficient to drive iron from the low-temperature bcc α phase to the fcc γ phase at $T_c^{\alpha\gamma}$, where $S^\gamma > S^\alpha$ (cf. the slopes of the relevant free-energy curves

in Fig. 2). It is only above the Curie temperature that the bcc magnetic disorder is sufficient for $S^{\delta} > S^{\gamma}$ and we find the transformation back from fcc to bcc structure at $T_c^{\gamma\delta}$. At the same time the relative stability of the hcp and fcc structures has reversed as the temperature rises through $T_c^{\epsilon\gamma}$ and the rms moment builds up. This change in relative stability accompanying the appearance of local moments is not altogether unexpected since even at absolute zero the nonmagnetic γ and ϵ structures would switch their relative stability[11,20] if they were to become (by lattice expansion) strong ferromagnets (cf. Fig. 9 of Ref. 11). Figure 1 shows the resulting phase diagram where under pressure the bcc α and δ phases become less stable compared to the close-packed γ and ϵ phases because the magnetic free energy has been reduced[11] compared to the nonmagnetic structural contribution.

The inclusion of the vibrational free energy would not change this *qualitative* picture. We have used Inden's[24] recent analytic expression for the magnetic specific heat of bcc iron to evaluate the *experimental* magnetic free energy. We find that its curvature is sufficient above $T_c^{\alpha\gamma}$ to take the system from the γ phase back to the δ phase without having to invoke any additional vibrational driving term, just as our calculation finds in Fig. 2. Moreover, Inden's[24] magnetic free energy clearly shows that SRMO, which we have neglected, cannot be responsible for the α to γ transformation since it leads to *increased* stability of the α phase by lowering the internal magnetic energy. However, our neglect of SRMO in the α phase does lead to the calculated Curie temperature T_C at $P=0$ occuring 90 K *above* the structural phase transition $T_c^{\alpha\gamma}$ rather than 140 K below. Yet experimentally[25] a pressure of only 18 kbar is required before the structural phase transition does indeed precede the second-order magnetic transition.

In conclusion, therefore, we have shown that the magnetic free energy drives the structural phase transitions in iron. We hope that the qualitative success of this simple model will encourage theorists to push the theory beyond the static, nondegenerate case and apply it to the many technologically important alloys of iron.

This work was started when one of the authors (H.H.) was visiting at Imperial College. He is much indebted to Professor E. P. Wohlfarth and Dr. D. M. Edwards for their warm hospitality and to the United Kingdom Science and Engineering Research Council for financial support.

[1]C. Zener, Trans. Am. Inst. Min. Metall. Eng. 203, 619 (1955).

[2]R. J. Weiss and K. J. Tauer, Phys. Rev. 102, 1490 (1956).

[3]D. Koski Maki and J. T. Waber, in *Electronic Density of States, Proceedings of the Third International Materials Research Symposium, Gaithersburg, Maryland, 1969,* edited by L. H. Bennett, National Bureau of Standards Special Publication No. 323 (U. S. GPO, Washington, D.C., 1971).

[4]L. Kaufman, E. V. Clougherty, and R. J. Weiss, Acta Metall. 11, 323 (1963).

[5]L. D. Blackburn, L. Kaufman, and M. Cohen, Acta Metall. 13, 533 (1965).

[6]G. Grimvall, Phys. Scr. 13, 59 (1976).

[7]Lin-gun Liu and W. A. Bassett, J. Geophys. Res. 80, 3777 (1975).

[8]H. Hasegawa, J. Phys. Soc. Jpn. 46, 1504 (1979), and Solid State Commun. 31, 597 (1979), and J. Magn. Magn. Mater. 15–18, 272 (1980).

[9]H. Hasegawa, J. Phys. Soc. Jpn. 49, 178 (1980), and 49, 963 (1980).

[10]J. Hubbard, Phys. Rev. B 19, 2626 (1979), and 23, 5974 (1981).

[11]See, for example, D. G. Pettifor, Calphad 1, 305 (1977).

[12]M. Cyrot, Phys. Rev. Lett. 25, 871 (1970); L. M. Roth, in *Transition Metals 1977,* IOP Conference Series Vol. 39, edited by M. J. G. Lee, J. M. Perz, and E. Fawcett (Institute of Physics, London, 1978), p. 473.

[13]P. Soven, Phys. Rev. 156, 809 (1967).

[14]T. Moriya, Solid State Commun. 26, 483 (1978).

[15]N. Beer and D. G. Pettifor, to be published.

[16]J. F. Janak and A. R. Williams, Phys. Rev. B 14, 4199 (1976).

[17]J. Küber, Phys. Lett. 81A, 81 (1981).

[18]J. Madsen, O. K. Andersen, U. K. Poulsen, and O. Jepsen, in *Magnetism and Magnetic Material—1975 (Philadelphia),* edited by J. J. Becker and G. H. Lander, AIP Conference Proceedings No. 29 (American Institute of Physics, New York, 1976), p. 327.

[19]V. Heine, Phys. Rev. 153, 673 (1969).

[20]D. G. Pettifor, in *Metallugical Chemistry,* edited by O. Kubaschewski (HMSO, London, 1972), p. 191.

[21]At equilibrium γ iron orders antiferromagnetically with a small moment of $0.7\mu_B$ and a Néel temperature of 67 K [G. J. Johanson, M. B. Mcgirr, and D. A. Wheeler, Phys. Rev. B 1, 3208 (1970)]. Since T_N is below room temperature and away from the interesting regions of the phase diagram, we do not consider the antiferromagnetic state here.

[22]The calculated free energies are those for the single band.

[23]At $T=0$ K we find a magnetic moment of $2.615\mu_B$, larger than the experimental $2.2\mu_B$ because of the neglect of *sd* hybridization.

[24]G. Inden, Physica (Utrecht) B103, 82 (1981).

[25]J. M. Leger, C. Loriers-Susse, and B. Vodar, Phys. Rev. B 6, 4250 (1972).